Conf-930676--11

Dependence of Debris Cloud Formation on Projectile Shape

C. H. KONRAD, L. C. CHHABILDAS, M. B. BOSLOUGH
Department 1433, Sandia National Laboratories
Albuquerque, New Mexico, 87185-5800

A. J. PIEKUTOWSKI, K. L. POORMON
University of Dayton Research Institute
300 College Park, Dayton, Ohio, 45469-0180

S. A. MULLIN, D. L. LITTLEFIELD
Southwest Research Institute,
6220 Culebra Road, San Antonio, Texas, 78228-0510

A two-stage light-gas gun has been used to impact thin zinc bumpers by zinc projectiles over the velocity range of 2.4 km/s to 6.7 km/s to determine the propagation characteristics of the impact generated debris. Constant-mass projectiles in the form of spheres, discs, cylinders and rods were used in these studies. Radiographic techniques were employed to record the debris cloud generated upon impact and the dynamic formation of the resulting rupture in an aluminum backing plate resulting from the loading of the debris cloud. The characteristics of the debris cloud generated upon impact is found to depend on the projectile shape. The data indicate that the debris front velocity is independent of the shape of the projectile, whereas the debris lateral/radial velocity is strongly dependent on projectile geometry. Spherical impactors generate the most radially dispersed debris cloud while the normal plate impactors result in column-like debris. It has been observed that the debris generated by the impact of thin plates on a thin bumper shield is considerably more damaging to a backwall than the debris generated by an equivalent-mass sphere.

INTRODUCTION

There has been considerable attention given to evaluate the effects of projectile shape in thick-plate penetration experiments. These studies have employed projectile shapes such as long rods or spheres. Very little data/analyses exist in which the penetration capability of debris resulting from impact of thin plates has been studied. In a computational study, it has been noted that the debris generated by the impact of thin plates on a thin bumper shield is considerably more damaging to a backwall than the debris generated by an equivalent mass sphere[1]. To determine these effects we have performed a series of systematic studies in which a constant mass zinc projectile impacts a thin zinc bumper sheet. The damage to a backwall plate resulting from subsequent loading by the debris generated by the bumper impact is measured. Zinc was selected in this study, because of its low melting and boiling temperature; it will melt and vaporize at relatively low impact velocities of 2.5 to 7 km/s. These experiments, combined with hypervelocity impact experiments in aluminum up to 11 km/s [2] will evaluate velocity scaling concepts [3].

EXPERIMENTAL CONFIGURATION

The experimental arrangement for the impact tests is illustrated in Figure 1. The zinc projectiles consisted of four different geometries—disk, sphere, cylinder and a rod. They made normal impacts on a thin zinc bumper plate. A 6061-T6 aluminum backwall was positioned 152.4 mm behind the zinc bumper. The mass of the projectiles was kept constant except in the case of a long rod. Fine source, soft x-rays were used to observe the projectile and the debris cloud formation resulting from impact [4]. As indicated in

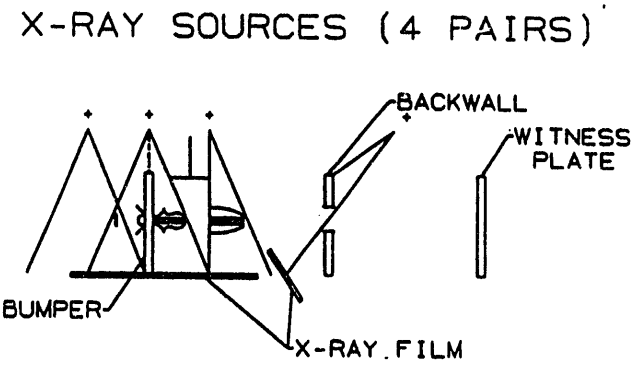

Figure 1. Experimental Impact Configuration

DISCLAIMER

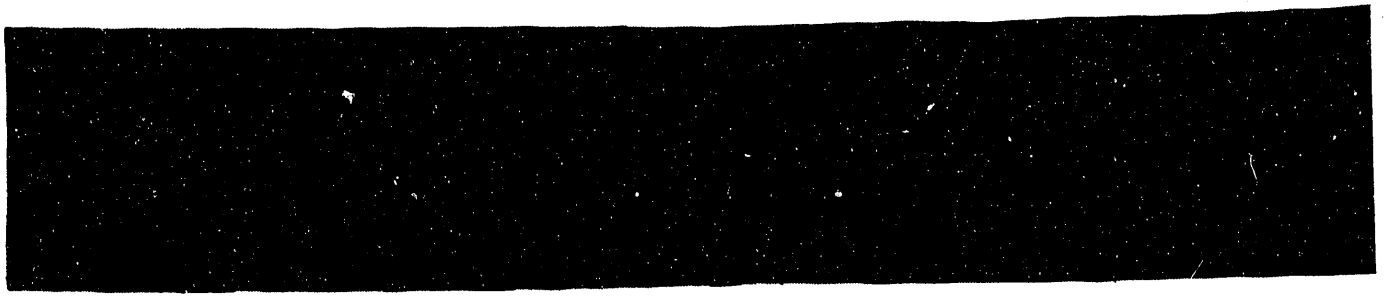

Figure 2a. The plate at left 5.9 μs before impact, and the debris cloud formation at 18.3 μs after impact. Dynamic hole formation is displayed at 51.2 μs after impact of the bumper plate and is compared to the hole size in the recovered plate at right.

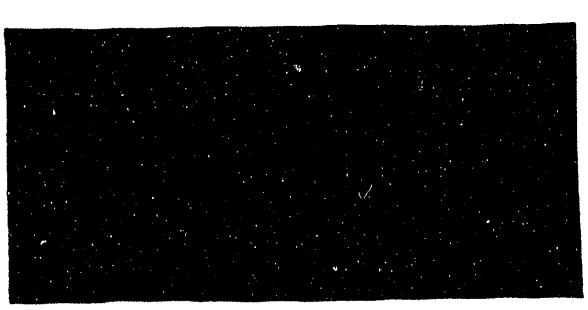

NO BACKWALL PENETRATION

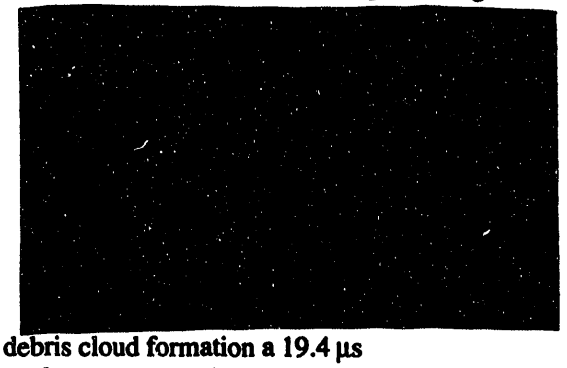

Figure 2b. The sphere at left 5.2 μs before impact, and the debris cloud formation a 19.4 μs after impact. No penetration of the backwall is achieved for the spherical impact.

Figure 2c. The cylinder at left 2.7 μs before impact and the debris cloud formation at 21.4 μs after impact. Dynamic hole formation is displayed at 49.4 μs after impact of the bumper plate and is compared to the hole size in the recovered plate at right.

Figure 2d. The rod at left 5.9 μs before impact and the debris cloud formation at 18.2 μs after impact. Dynamic hole formation is displayed at 51.2 μs after impact of the bumper plate and is compared to the hole size in the recovered plate at right.

Table 1. Summary of Experiments

Shot No.	Impactor Shape	Impactor Dimensions diam. x thick. (mm mm)	Impactor Mass (gm)	Impactor Velocity (km/s)	Front Velocity (km/s)	Lateral/ Radial Velocity (km/s)	Bumper Hole Size diam. x diam. (mm x mm)	Dynamic Hole Size diam. x diam. (mm x mm)	Recovered Hole Size diam. x diam. (mm x mm)
1511	Plate	13 x 0.759	0.731	5.01	5.22	0.92	20 x 20	14.5 x 13.5	14.5 x 13.5
1515	Sphere	5.77	0.719	4.98	4.71	2.84	12.0 x 11.4	No Hole	No Hole
1553	Cylinder	5.05 x5.05	0.716	5.22	5.22	Tilted	14.4x14.4 Torn	6.1 x 50	26.2x56.1
1554	Rod	3.98 x 14.2	1.241	4.97	5.28	1.93	10.1 x 10.1	38.1x36.3	35.6x35.6

Figure 2, the projectile orientation is determined prior to bumper plate impact. In addition, the debris cloud formation at ~ 19 μs after impact is also indicated. (Multiple exposures were taken to determine the debris evolution but are not displayed in Figure 2.) Radiographic measurements of the backwall were also made during the experiment to determine the *in-situ (i.e., the dynamic)* formation of a hole in the backwall. This x-ray was exposed at an oblique angle.

RESULTS

The summary of the experiments reported in this paper is given in Table 1. A detailed summary of all experiments conducted is reported elsewhere [5]. Multiple exposures taken to determine the debris cloud evolution are also reported in reference 5. Figure 2 indicates the debris cloud evolution for different projectile shapes at ~ 19 μs after impact.

The debris front velocity indicated in the table is an average of the three different radiographic measurements taken at three different times [5]. Likewise, the lateral velocity reported in the paper is determined at the maximum

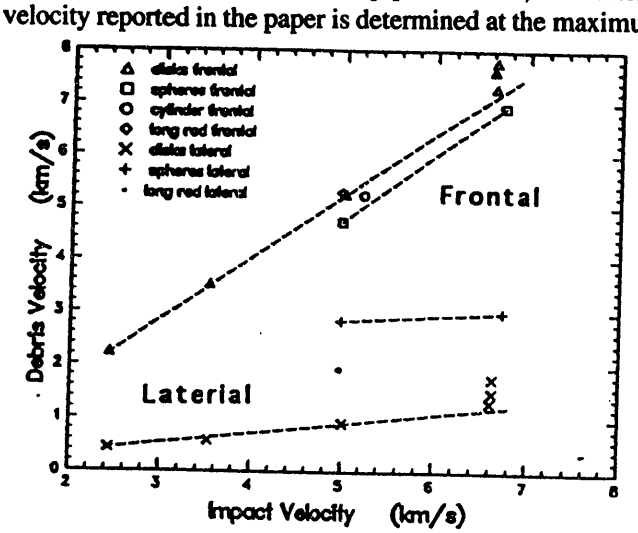

Figure 3. Debris Front and Lateral Velocity variation with impact velocity for all projectiles

radius of the debris cloud as determined by the multiple x-ray exposures. It represents the rate of change of radius with time. The debris front velocity and the lateral velocity are displayed in Figure 3 for all experiments performed in this investigation.

The hole size in the recovered backwall plate (see Table 1) are indicated in Figure 4 for plate and spherical projectiles as a function of impact velocity. The hole size shown in Figure 4 is transformed to an equivalent areal dimension. The hole size in the bumper plate is also given in Table 1. Because the impactor in the cylinder experiment is considerably tilted prior to impact, the hole size is not symmetrical as in the other experiments, and the bumper is torn.

DISCUSSIONS

Size and Shape Dependence of the Debris Cloud

The debris clouds generated upon impact of different projectiles are indicated in Figure 2. As summarized in Table 1, these experiments were performed for a constant

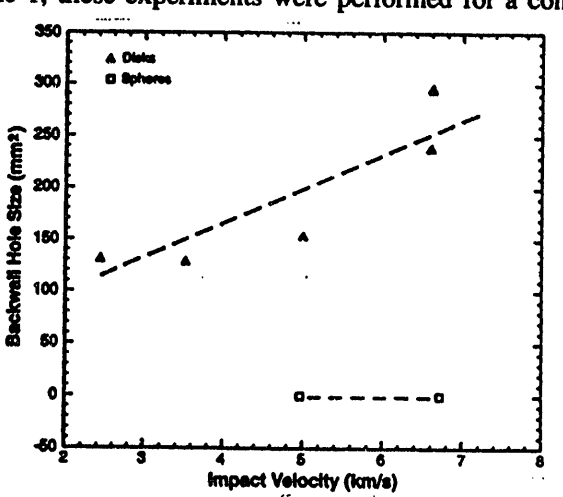

Figure 4. Backwall hole size as a function of impact velocity for plate and spherical projectiles.

mass projectile and at an impact velocity of ~ 5 km/s. For plate impact, the distinct features of the observed debris cloud consist of a leading edge resembling a high density plate followed by a lower density column over the remaining length. The shape of the debris cloud is tilted similar to the impactor tilt angle. The central column does not appear to radially expand with time, suggesting the one-dimensional nature of propagation for the central column. The central column is surrounded by a lower density cloud which is presumably vapor. The lateral dispersion for the plate impact is the least when compared to the debris cloud generated by other projectile shapes. This is graphically illustrated in Figure 3 where the radial velocity for the plate is the lowest of all the other projectile shapes. Since the cloud has not dispersed sufficiently, this central column is quite detrimental when it interacts with the backwall.

The debris cloud in Figure 2b is for a spherical impact configuration with a similar mass at the same velocity. The debris cloud has a high-density diffused leading edge that is considerably dispersed within the debris cloud. Two-dimensional effects resulting from the impact of the sphere and bumper shield disperses the debris cloud more efficiently, and imparts a large radial velocity component. This is indicated in Figure 3. For this reason, the backwall is not penetrated due to the spherical nature of the debris cloud, since the impulse is spread over a larger surface area of the backwall.

Figures 2c and 2d show the debris cloud that results from impact of a cylinder(L/D=1) and a rod(L/D=3.6). Even though the masses of the two projectiles are not identical, some features of the debris cloud appear to be common to both. They both have a distinct conical leading edge separated from the spherical debris cloud. In the case of the cylinder, it sees sufficiently high loading stresses resulting in total fragmentation; however, due to stress attenuation effects in the long rod the back end of the rod remains intact. This results in a remnant rod, travelling unperturbed at the impact velocity, as indicated in Figure 2d. (There are also some solid fragments along the periphery of the spherical front which are not clearly distinguishable in Figure 2d.)

In both the examples shown in Figures 2c and 2d, the backwall is ruptured. As a result of significant tilt for cylinder impact, the backwall appears to be torn. It is anticipated that rupture would have occurred under ideal impact conditions [6], but with a smaller hole compared to plate impact since the debris cloud in Figure 2c appears to be dispersed. The experiment needs to repeated to address this issue. It is not surprising that a rupture was caused by the debris generated in the long rod impact of Figure 2d. The remnant rod in the debris cloud travelling at 5 km/s can cause the backwall structure to rupture; this is further compounded by solid fragments that are also present in the debris.

Debris Velocities

Figure 3 shows the propagation characteristics of the debris cloud that are indicated in Figure 2. In all experiments, the leading edge of the debris front (defined as the frontal velocity) is traversing at the impact velocity. The lateral velocity, however, is more dependent on the impactor geometry. For the debris cloud formed by the plate impact the lateral velocity was 0.92 km/s (~ 18% of the impact velocity) while the sphere impact had a lateral velocity of 2.84 km/s (~ 57% of the impact velocity). As mentioned before, one dimensional effects dominate the debris cloud propagation processes in plate impact geometry, while two-dimensional effects influence the spherical impact configuration, resulting in a large lateral velocity component. No lateral velocity could be obtained for the cylinder impact because the skewed debris cloud resulting from the tilted impact made measurements difficult. The rod lateral velocity of 1.93 km/s (~ 39% of the impact velocity) falls between the plate and the disk.

ACKNOWLEDGMENTS

This work performed at Sandia National Laboratories supported by the U.S. Department of Energy under contract DE-AC04-76DP00789. We would also like to acknowledge Tom Tsai and John Connell, Defense Nuclear Agency for their interest and partial support provided for this work.

REFERENCES

[1] E. S. Hertel, L. C. Chhabildas, L. Yarrington, "Computational Determination Of Ballistic Limits For A Simple Whipple Bumper Shield," in *Proceedings of the Workshop on Hypervelocity Impacts in Space-1991*, ed. by J. A. M. McDonnell, 1992, pp. 15-18.

[2] L. C. Chhabildas, M. B. Boslough, W. D. Reinhart, C. A. Hall, "Debris Cloud Characterization at Impact Velocities over 5 to 11 km/s", this volume.

[3] S. A. Mullin, D. L. Littlefield, C. E. Anderson, Jr., N. T. Tsai, Velocity Scaling of Impacts into Spacecraft Targets at 8 to 15 km/s, private communication.

[4] A. J. Piekutowski, *Intl. J. Impact Engng.*, V10, pp. 453-471, (1990).

[5] C. H. Konrad, L. C. Chhabildas, M. B. Boslough, A. J. Piekutowski, K. L. Poormon, S. A. Mullin, D. L. Littlefield, Sandia National Laboratories Report (unpublished).

[6] R. H. Morrison, "A Preliminary Investigation Of Projectile Shape Effects In Hypervelocity Impact Of Double-sheet Structures," NASA Technical Note NASA TN D-6944, 1972.

END

DATE
FILMED
10/6/93